Spatial super-resolution differential confocal microscopy based on radial birefringent pupil filter

Zou Limin[1,2,#], Hou Siliang[2] and Fan Zhigang[1]

1 Postdoctoral Research Station of Optical Engineering, Harbin Institute of Technology, Harbin 150001, China
2 Institute of Ultra-precision Optoelectronic Instrument Engineering, Harbin Institute of Technology, Harbin 150080, China
Corresponding Author / E-mail: zoulimin@hit.edu.cn., TEL: +86-451-86412896, FAX: 0451-8641-2698

KEYWORDS : Radial birefringent pupil filter, pupil function, differential confocal, Super-resolution

In order to improve the spatial resolution of a confocal system, a lateral birefringent pupil filter is introduced into a differential confocal system which consists of two polarizers and a birefringent element between them. The expression of the pupil function is deduced using Jones algorithm. The size and position of the birefringent pupil filter are optimized by analyzing the first zero ratio, one of the most important parameters. Lateral super-resolution can be realized by changing the direction of the polarizer in the radial birefringent pupil filter and the angle between the axis of the birefringent element and the optical axis. A maximum improvement of axial super-resolution can be realized by detecting the difference between the signals coming from two optical paths. The results of theoretical analysis and preliminary experiment indicate that the optimized pupil filter can be used to bring the axial resolution up to 3nm and to significantly improve the lateral resolution while the lateral size deviates from the standard step by 0.27μm . The spatial resolution of imaging and detecting can be further improved by introducing radial birefringent pupil filter into a confocal system.

Manuscript received: January XX, 2011 / Accepted: January XX, 2011

1. Introduction

Since the 50s of last century, when it was first brought up by M. Minsky, the confocal microscopy technology has been widely applied in biomedicine, micro-electronics, and material science, due to its high resolution and unique chromatographic ability. However, a traditional confocal system could not satisfy the high resolution requirement of imaging and detecting. With the development of very-large-scale integration (VLSI) of semiconductor and the micrometer or quantum devices, micro fabrication has reached the deep sub-micron and nano 3-D process stage[1]. Lateral deep sub-micro and axial nano high spatial resolution have become an important objective to be achieved in present confocal field.

Nowadays, introducing pupil filtering technology into confocal microscope technology to realize super-resolution is the most effective way to achieve optical super-resolution imaging[2-7]. Differential confocal detecting technology, complex dynamic color confocal technology and dephasing detecting technology were put forward to realize higher axial resolution[8]. In order to satisfy the requirement of lateral high resolution, the research of "Spatial Super-resolution Differential Confocal Microscopy based on Radial Birefringent Pupil Filter (SSDCM based on RBPF)" is proposed in this paper by introducing an optimized radical birefringent super-resolution pupil filter into a differential confocal system, and deducing the expression of the pupil function using Jones algorithm; Lateral super-resolution can be realized by changing the angle between the direction of the polarizer in the radial birefringent pupil filter and the optical axis of the birefringent element; while the axial super-resolution can be improved by differential detection of dual optical path.

2. Principle of SSDCM based on RBPF

As shown in Fig.1 and Fig.2, filter can be placed in position A, B and C[9-10]. The radial refringent filter is composed of two polarizers and a birefringent element between them. Supposed the radius of curvature of the spatial birefringent element is R (R<0), and the minimum thickness of the element as d0. Its fast axis is defined as the optical axis, and the angle between the optical axis and x axis as θ. Thus, Jones matrix of the birefringent element could be expressed as shown below:

$$L=\begin{pmatrix} \cos[\frac{\sigma(r)}{2}]-i\sin[\frac{\sigma(r)}{2}]\cos(2\theta) & -i\sin[\frac{\sigma(r)}{2}]\sin(2\theta) \\ -i\sin[\frac{\sigma(r)}{2}]\sin(2\theta) & \cos[\frac{\sigma(r)}{2}]+i\sin[\frac{\sigma(r)}{2}]\cos(2\theta) \end{pmatrix} \quad (1)$$

Where Δn is the difference of the birefringent materials, λ is the

wavelength of incident light. d(r) is the thickness the birefringent element at r. According to the Jones algorithm, the pupil function of the radial birefringent filter could be deduced as:

$$P(r)=\cos[\frac{\sigma(r)}{2}]-i\sin[\frac{\sigma(r)}{2}]\cos(2\theta) \tag{2}$$

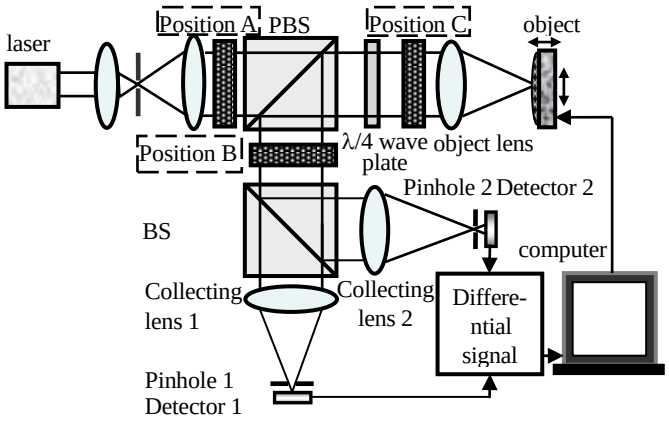

Fig. 1 Schematic diagram of differential confocal microscopy based on pupil filter

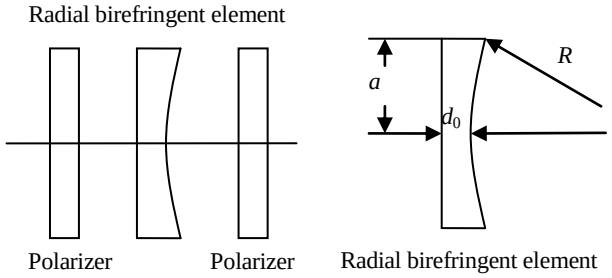

Fig. 2 Diagrammatic sketch of radial birefringent filter and radial bire fringent element

In order to apply the spatial birefringent element as a half-wave plate along axis z, and a full-wave plate at position a away from axis z, the unknown parameters of the pupil function are a and θ, which are the size of filter and the angle between x axis. By evaluating the parameters of super-resolution characteristics, it can be found that when θ=π/4, the first zero coordinate G, one of the parameters, has its minimum. The relationship between a and G can be obtained by defining the first zero ratio. Considering the probability of processing, a=7 is assigned. Thus the parameters of birefringent element are obtained, d_0=5.673mm, d_a=5.730mm, R=-427.55mm. So the pupil function is obtained as shown below:

$$P(r)=\cos[8.725\pi(5.763+\frac{r^2}{855.1})] \tag{3}$$

We may also obtain the intensity response function I(v,u) of the whole system:

$$\begin{aligned} I(v,u)=&\left|[\int_0^1 P_{1L}(\rho)e^{\frac{iu\rho^2}{2}}J_0(\rho v)\rho d\rho]\cdot[\int_0^1 P_{2L}(\rho)e^{\frac{i(u-u_M)\rho^2}{2}}J_0(\rho v)\rho d\rho]\right|^2 \\ &-\left|[\int_0^1 P_{1L}(\rho)e^{\frac{iu\rho^2}{2}}J_0(\rho v)\rho d\rho]\cdot[\int_0^1 P_{2L}(\rho)e^{\frac{i(u+u_M)\rho^2}{2}}J_0(\rho v)\rho d\rho]\right|^2 \end{aligned} \tag{4}$$

Where L stands for positions A, B, and C; u_M is the axial deviation of a detector; and the pupil functions of object lens and the collecting lens are $P_1(\rho)$ and $P_2(\rho)$ respectively; $J_0(\rho v)$ is the zero-order Bessel function; ρ is the normalized radius, and ρ=r/a; a is the size of a lens; r is the radial coordinate and z is the radial defocusing amount.

From Eq.(3), the pupil functions of object lens and collecting lens can be obtained when the pupil filter is placed at position A, B or C in the system.

Position A:

$$P_{1A}(\rho)=P_{2A}(\rho)=\begin{cases}\cos[8.725\pi(5.763+\frac{(5\rho)^2}{855.1})] & 0\le\rho\le1\\ 0 & \rho\ge1\end{cases} \tag{5}$$

Position B:

$$P_{1B}=\begin{cases}1 & 0\le\rho\le1\\ 0 & \rho\ge1\end{cases} \tag{6}$$

$$P_{2B}=\begin{cases}\cos[8.725\pi(5.763+\frac{(5\rho)^2}{855.1})] & 0\le\rho\le1\\ 0 & \rho\ge1\end{cases} \tag{7}$$

Position C:

$$P_{1C}=\begin{cases}\cos[8.725\pi(5.763+\frac{(5\rho)^2}{855.1})] & 0\le\rho\le1\\ 0 & \rho\ge1\end{cases} \tag{8}$$

$$P_{2C}=\begin{cases}\left\{\cos[8.725\pi(5.763+\frac{(5\rho)^2}{855.1})]\right\}^2 & 0\le\rho\le1\\ 0 & \rho\ge1\end{cases} \tag{9}$$

2.1 Lateral Response of SSDCM based on RBPF

According to (4)-(9), the distribution of lateral response intensity can be obtained when the object of the system is on the focal plane of object lens, and there is no deviation in detector:

$$\begin{aligned} I(v,0)=&|[\int_0^1 P_1(\rho)J_0(v\rho)\rho d\rho]\prod[\int_0^1 P_2(\rho)J_0(v\rho)\exp(-\frac{iu_M\rho^2}{2})\rho d\rho]|^2 \\ &-|[\int_0^1 P_1(\rho)J_0(v\rho)\rho d\rho]\prod[\int_0^1 P_2(\rho)J_0(v\rho)\exp(\frac{iu_M\rho^2}{2})\rho d\rho]|^2 \end{aligned} \tag{10}$$

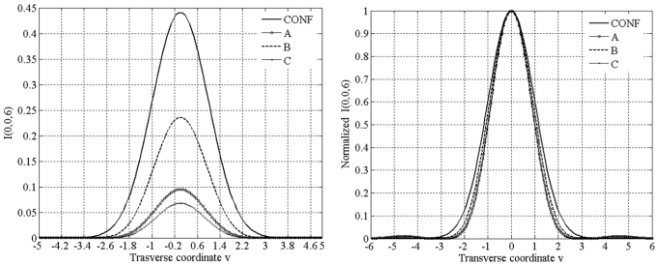

a) lateral response intensity b) normalized lateral response intensity

Fig.3 Relationship between lateral response intensity and pupil position

It can be seen from Fig.3 that the system can be used to realize lateral super-resolution in three positions; but its characteristics vary with positions and defocusing amounts. The lateral resolution of the system reaches its minimum when there is no filter at all, but the response intensity is the highest. In position B, the response intensity is the highest, while the lateral resolution is still higher than the one when there is no filter. In position C, the response intensity is the minimum and the lateral resolution is the highest. In position A, the response intensity is higher than that of position C, and the resolution is higher than that of position B; the resolution at A and C is nearly the same.

2.2 Axial Response of SSDCM

When the detectors have a defocusing amount, the axial response function of SSDCM can be expressed as below:

$$I(0,u,u_M)=|[2\int_0^1 P_1(\rho)\exp[-\frac{iu\rho}{2}]\rho d\rho]\times[2\int_0^1 P_2(\rho)\exp[-\frac{i(u-u_M)\rho}{2}]\rho d\rho]|^2 - |[2\int_0^1 P_1(\rho)\exp[-\frac{iu\rho}{2}]\rho d\rho]\times[2\int_0^1 P_2(\rho)\exp[-\frac{i(u+u_M)\rho}{2}]\rho d\rho]|^2 \quad (11)$$

It can be seen from Eq.(11) that the axial response intensity function has relations with the defocusing amount and the position pupil filter placed. When the parameters of a pupil filter are fixed, the axial response function of SSDCM is a binary function of normalized axial coordinate u and axial deviation u_M. When axial deviation u_M=5.21, the axial response curves of the pupil filter is as shown in Fig.4.

It can be seen from Fig.4 that when the pupil filter is placed in a different position, the axial response curves of differential confocal imaging system vary. In summary, after introducing the pupil filter, axial response curves become worse.

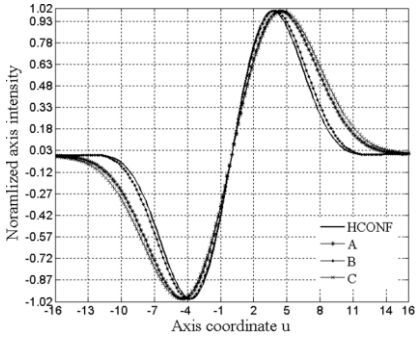

Fig.4 Relationship between axial intensity and position of filter

2.3 Experiment and Analysis

The experimental set-up of SSDCM is based on the principle shown in Fig.1. During the experiment, a liquid crystal spatial modulator (SLM) based on birefringent principle was used to simulate the pupil filter placed in position A. And the correlative phase-modulation could be carried out on a grey-scale map.

2.3.1 Experimental Analysis of Axial Response

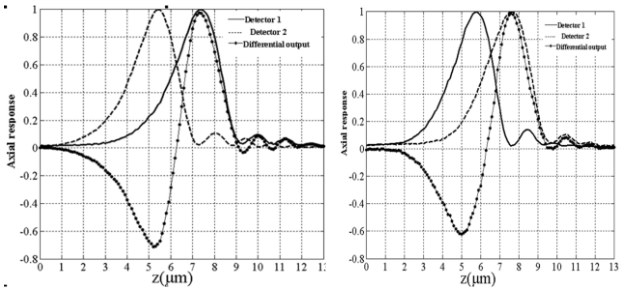

a) without pupil filter element b) with pupil filter element

Fig.5 Experimental axial response of the differential confocal system

It can be seen from Fig.5 a) and b) that the linearity of axial intensity response curve after differential is much better than that of the single path. Within its focusing range, the axial response curve has its rate of slope twice higher and has an absolute zero point.

As shown in Fig.6, birefringent pupil filter placed in position A will cause a little decrease in the axial characteristics of the super-resolution differential confocal system.

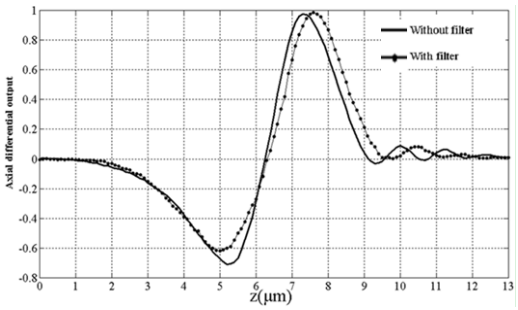

Fig.6 Comparison of axial response curves of pupil differential confocal microscopic systems

In order to test the axial resolution of pupil differential confocal microscopy system simulated by a liquid crystal spatial modulator, we used P-517.3CD inching operating platform to make a traverse motion periodically along axis z, to make sure that the measuring system can recognize the periodical traverse motion as a criterion to test the axial effective resolution. Shown in Fig.7 is the resolution test curve of the axial resolution of differential confocal system with or without birefringent pupil filter.

By comparing Fig.7 a) and b), we can see that, for a differential confocal system, when the step length is 3nm or 2nm, the system can recognize the surface periodical traverse motion forward or backward correctly; when the step length is 1.5nm, the experimental curve presents mistakes about the direction in some places. Therefore, we can regard the axial resolution of the system is 2nm. For the super-resolution pupil confocal microscopy system, when the step length is 4nm or 3nm, the system can recognize the surface periodical traverse motion forward or backward correctly; when the step length is 2nm, there are several mistakes about the direction from the third data point in the experimental curves. Thus, we think the axial resolution of the system is 3nm.

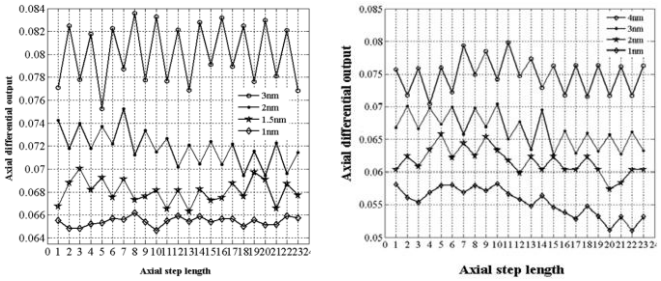

a) without the pupil filter element b) with the pupil filter element

Fig.7 Experimental curve of axial resolution of pupil differential confocal system

2.3.2 Experimental Analysis of Lateral Response

During the experiments, we used TGZ1-PTB grating as a standard step to test the lateral resolution of the system, which is a grating structure with a period of 3±0.01μm, and a height of 21.3±0.9nm.

As shown in Fig.8, the coordinate in the position of 1/4 height of the step response from A to B and the one from C to B, are (3.547, 0.2848) and (5.232, 0.2796), respectively. The separation of their horizontal ordinate is 1.685μm, with a deviation of 0.185μm which is comparable to 1.5μm shown in the TGZ1-PTB certification. That is to say, the deviation from the lateral width of standard step is 0.19μm, if NA=0.75, when the laser source with wavelength of 632.8nm is used. As shown in Fig.8, the coordinate in the position of 1/4 height of the

step response from D to E and the one from F to E, are (3.514, 0.3197) and (5.28, 0.2576), respectively. The separation of their horizontal ordinate are 1.746μm, with an extra 0.266μm which is comparable to what is shown in TGZ1-PTB certification. In summary, under the same condition, the lateral resolution of the system can be greatly improved by introducing the birefringent filter.

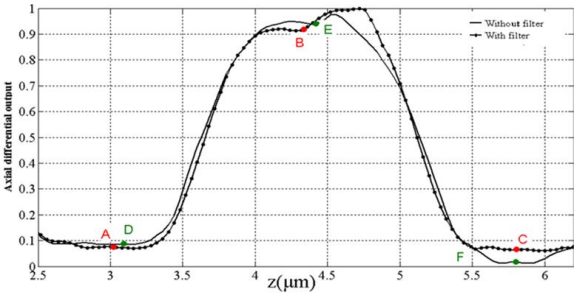

Fig. 8 Comparison of scanning curves of the step during the experiment

3. Conclusions

Contents In order to improve the resolution of our optical system, by combining the super-resolution pupil filtering technology and the differential confocal microscopy, the super-resolution differential confocal sensing method and technology based on the birefringent principle are carefully studied. In order to suppress the side lobe and to have a high axial resolution, we introduce a specially designed radial birefringent pupil filter into differential confocal system, to enable the system to realize 3-D super-resolution. The imaging characteristics of the super-resolution differential confocal microscopy with a birefringent pupil filter are discussed in detail, especially the super-resolution character and the response sensitivity with the filter placed in different positions. Experimental results indicate the effectiveness of the super-resolution ability of the system. Seen from the result, the lateral characters of the system can be improved by introducing the birefringent element. However, due to the influence of the performance parameters of a liquid crystal spatial modulator, there is much room for further improvement of the lateral characters of the system when a real birefringent element is introduced.

ACKNOWLEDGEMENT

This work was supported by the Youth Fund of Heilongjiang Province under Grant QC2009C11, the China Postdoctoral Science Foundation funded project under Grant 20100471083 and the National Natural Science Foundation of China under Grant 51075084.

REFERENCES

1. S. Zhou, C. Zhou. Discrete Continuous-phase Super-resolution Filters. Opt. Lett. 2004, 29:2746~2748
2. Partha. P. Mondal, Alberto Diaspro. Lateral resolution improvement in two-photon excitation microscopy by aperture engineering. Opt. Commun. 2008, 281 (7):1855-1859
3. B.R. Boruah. Lateral resolution enhancement in confocal microscopy by vectorial aperture engineering. Appl. Opt. 2010, 49 (4):701~707
4. Gong Wei, Si Ke, Sheppard. Colin J. R. Optimization of axial resolution in a confocal microscope with D-shaped apertures. Appl. Opt. 2009, 48(20): 3998~4002
5. S. F. Pereira, A. S. van de Nes. Super-resolution by Means of Polarization, Phase and Amplitude Pupil Masks. Opt. Commun. 2004, 234: 119~124
6. Ngoc Diep Lai, Jian Hung Lin, Po Wen Chen, Jaw Luen Tang, Chia Chen Hsu. Controlling Aspect Ratio of Focal Spots of High Numerical Aperture Objective Lens in Multi-photon Absorption Process. Opt. Commun. 2006, 258(2): 97~102
7. Jason B. Stewart, Bahaa E. A. Saleh, Malvin C. Teich, John T. Fourkas. Experimental Demonstration of Polarization-assisted Transverse and Axial Optical Super-resolution. Opt. Commun. 2004, 56:315~319
8. Zhao Weiqian, Tan Jiubin, Qiu Lirong. SABCMS, A New Approach to Higher Lateral Resolution of Laser Probe Measurement. Sensors and Actors A. 2005, 120(1): 17~25
9. Zou Limin, Li Xi, Zhang Hongji, Ding Xuemei. Improvement of Lateral Resolution Property of Differential Confocal System using Radial Birefringent. Proceedings of the SPIE 2008, 7133:71330-713340
10. Yun Maojin, Liu Liren, Sun Jianfeng, Liu Dean. Research on Super-resolution of Radial Birefringent Filter. ACTA OPTICA SINICA. 2005, 25(1):131-135